

# Procedure to deposit Gold only on the sidewalls of rectangular nanostructures and its applications

Zain Zaidi\*, Saara Khan\*, James Conway, J Provine, Michelle Rincon, Roger Howe  
Stanford University, USA

E-mail: szzaidi@stanford.edu and saarak@stanford.edu

\* = primary authors

June 6, 2014

## Abstract

This paper describes the implementation of sidewall metal deposition for Germanium nanobeams and Silicon Nitride strip waveguides. This methodology can be robustly applied to various structures with minimal changes to the overall process. Here we primarily use an e-beam metal evaporator, and Argon sputter etch as our main processes to achieve the desired result.

## 1 Introduction

The first demonstration of nanometer-scale sidewall formation was explored and developed for dry-etching-based pattern transfer techniques in 1989 by VanZeghbroech [1]. In this work, silylation of organic resist rendered resist much more resistant to oxygen RIE and plasma etching than other processes. This allowed for anisotropic RIE with oxygen to proceed slowly through the silylated layer on top of the structure and continue much more quickly in the unsilylated resist to leave behind free-standing sidewalls after etching.

More recent work has described a method to conduct sidewall lithography using Au nano-sidewalls through a multi-step process using sputtering, anisotropic sputter etching, dry etching by DRIE, and hot embossing [2]. The goal of this technique is similar to VanZeghbroech's work in that it also aims to have free standing nanostructures. In our work we aim to achieve sidewall metal deposition, not for achieving free standing nanostructures, but rather for the purpose of having clean metal sidewalls adhere to a nano- or micro- beam.

This work presents the first demonstration of a

procedure of sidewall metal depositions using angled electron beam evaporation and argon sputter etching. The sidewall thickness and surface profile was investigated by varying etch times and is confirmed using SEM imaging. We then apply this technique to SiN waveguides and Ge nanobeams to test some applications from making structures using this technique.

## 2 Experimental Procedures

The mechanism to fabricate structures with metal only on the sidewalls requires two steps: metal deposition with significant sidewall coverage, and normally incident dry etching.

### 2.1 Metal Deposition

We explored two techniques to deposit metal: a sputtering system, and an e-beam evaporation system. We compared the sidewall metal coverage in both of these tools and then selected the technique with the most conformal sidewall coverage. We used the Innotec ES26C e-beam evaporator in Stanford

Nanofabrication Facility (SNF) for depositing metal through the evaporation technique. Due to the nature of e-beam evaporator, metal deposition in such systems is expected to be very directional and metal is evaporated in a parabolic shape. Wafers are thus placed on a parabolic planetary on top so that metal is deposited at a normal incidence to the wafers. This is illustrated in the Fig. 1.

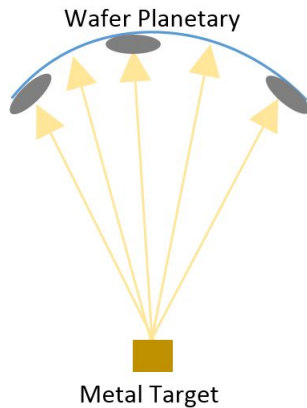


Figure 1: Schematics of an e-beam evaporator system

Although the shape of the wafer planetary is configured to minimize sidewall coverage, angled mounts can be attached to the planetary to enhance it. With the angled mount, the evaporated metal is incident at an acute angle to the normal of the wafer. Thus metal is deposited at an angle and allows for significant sidewall coverage. This is illustrated in Fig. 2.

In Innotec, we used the angled holder to mount our wafers. The actual image of our mounting setup is shown in Fig. 3.

Metal deposition with good sidewall coverage on both sides can then be achieved by rotating the wafer by a 180 degrees and depositing again.

Unlike an e-beam evaporator tool, metal sputtering tools are cruder and not directional. A metal target is bombarded by energetic ions, and metallic atoms that are ejected from the target are then sputtered on to the wafer. We used the Metalica Sputter System in the SNF. The mechanism of a metal sputtering system is depicted in Fig.4.

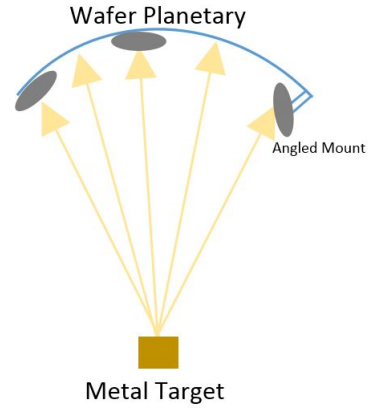


Figure 2: Schematics of an e-beam evaporator system with an angled mount



Figure 3: Angled mount configuration that we used in Innotec for our depositions

Due to the nature of this technique, sidewall step coverage is always expected. However, it is difficult to control and more random in nature. A key advantage in using this technique is that double deposition is not necessary to get metal coverage on both sidewalls. Another advantage is that there is no need of an angled mount.

## 2.2 Normally Incident Dry Etching via MRC

After depositing metal through the e-beam evaporator or the sputtering system, we then etched our



Figure 4: Schematics of a sputtering metal deposition system

samples in a way such that only the metal on the horizontal surfaces would get etched. While mechanisms have been developed to wet etch gold, such etching mechanisms tend to be isotropic in nature and do not conform our needs [3]. Argon sputter etching is a commonly used mechanism to etch a wide variety of materials. Argon atoms are bombarded on surface, and they eject the atoms on target as they strike. Under specific conditions, this etch is very directional, and Argon atoms strike the wafer at normal incidence. Etching under such a configuration would result in Gold being etched only from all the horizontal surfaces, thus leaving Gold only on the sidewalls.

We used the MRC Model 55 RIE, a plasma reactive ion etching system, in the SNF to perform the Argon sputter etching. We varied specific parameters (etch time, RF power, chamber pressure) while keeping other parameters constant (Argon flow) to get the desired result.

The idea of how this technique works is via two angled depositions using the an e-beam metal evaporator tool or at normal incidence in metal sputter systems. The metal deposition is then followed by Argon sputter etching in MRC. The goal is to remove all of the metal from the surface of the rectangular nanostructures except at the sidewalls of the structures. The system schematic of this procedure

is shown in Fig. 5

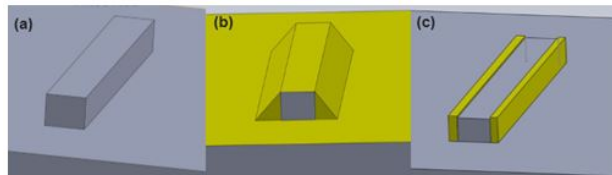


Figure 5: An illustration of the metal deposition with significant side wall coverage and the normally incident dry etching

For a single innotec angle deposition as described previously for 50 nm of gold, we performed several iterations of parameter changes to find the optimal sidewall coverage. Standard recipes for the MRC suggest Ar gas at 15sccm, chamber pressure 12mT, RF power at 100W, and peak voltage at 660V for a gold etch of 90A/min. Based on the standard recipe we started iterations of power at 100W. We then varied RF power between 80-100W, but found the etch rate was too fast to optimize for achieving clean gold sidewalls and led all samples to etch nondirectionally as shown in Fig. 6

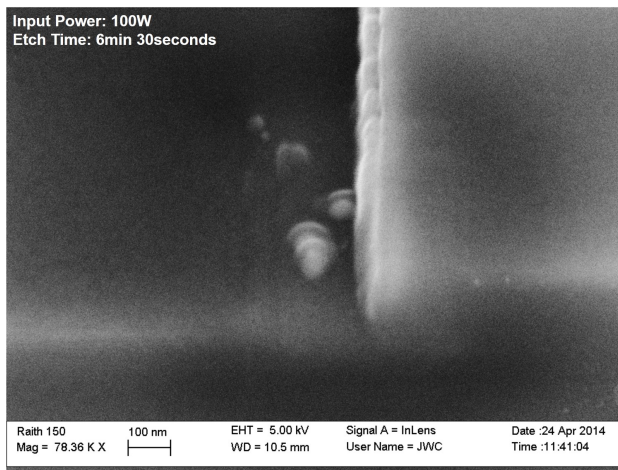


Figure 6: Results of nondirectional gold etching in the MRC due to high input powers. Sidewalls appear to be very thin.

We found that at a RF power of 70W we had bet-

ter control over various etch times to find optimal timing for sidewall etch control. At 70W, we varied etch times between 180-300 seconds. Times below 220 seconds still had a thin layer of gold on the surface. Times above 230 seconds looked completely etched from a 50x objective in a standard microscope. A SEM was then used to verify if there was any gold still present on the surface or sidewalls. From the SEM we found that times under 290 seconds still contained a very thin film of gold on the surface as shown in Fig. 7

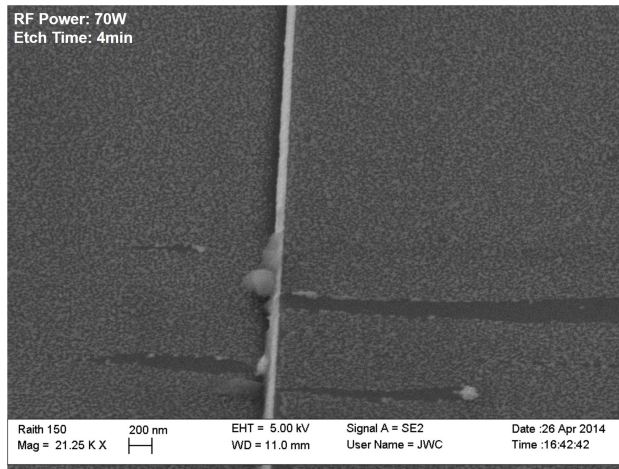


Figure 7: Gold was still present on the surface at 240 seconds (4minutes) and was found to still be on the surface for etch times below of 290 seconds for RF power of 70 Watts

Fig. 8 shows that at 300 seconds the gold film has been completely removed from the surface and a robust layer of 50nm of gold has been deposited on the sidewalls. Once this time was found for an Innotec angled deposition of 50nm, it was found to be repeatable with the same chamber conditions.

For a double angled Innotec deposition for 100nm of gold for each deposition, we found optimal MRC conditions after repeating several etch time iterations. For system conditions of the following: Ar gas at 15sccm, chamber pressure 12mT, RF power at 70W, and peak voltage at 660V, we varied the etch times between 540 seconds to 720 seconds (9 to

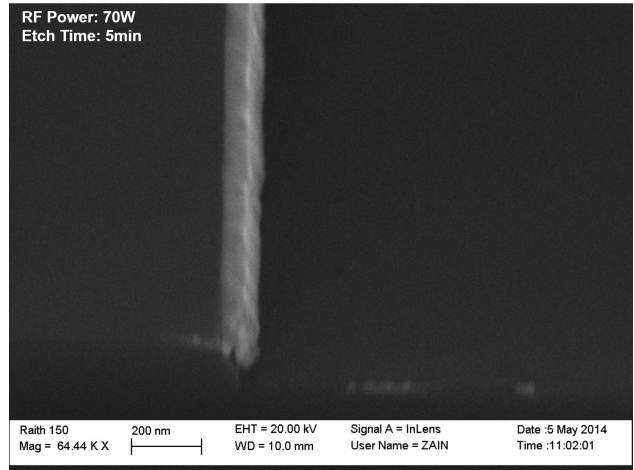


Figure 8: All gold from surface has been removed at 300 seconds (5minutes) and 50nm sidewalls are present on the edge of the sample

12 minutes) and found 600 seconds to be the optimal etch time for obtaining gold sidewalls with no gold present on the surface. We found for etch times above the optimal etch time of 600 seconds, the gold sidewalls were still present but began to become shallower and show in Fig. 9

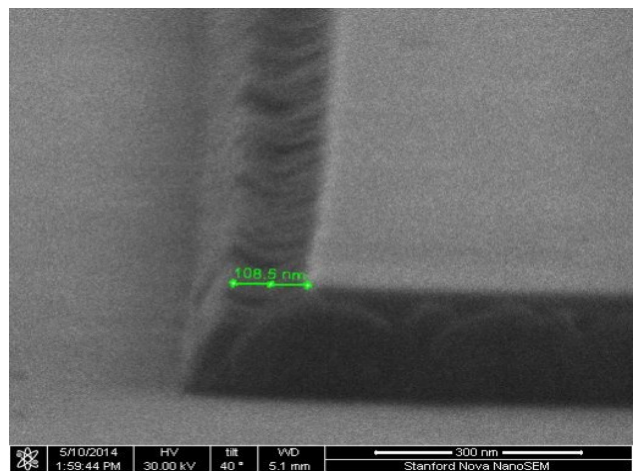


Figure 9: Gold sidewalls begin to show signs of overetching due to Argon bombardment at 720 seconds (12 minutes)

Fig. 9 shows the importance of finding the best etch rate for sidewall metal depositions based on the amount of metal deposited. In this section we showed that for a single angled deposition in the Innotec of 50nm has optimal etching condition in the MRC for 300 seconds (5minutes) at Ar gas at 15sccm, chamber pressure 12mT, RF power at 70W, and peak voltage at 660V. For double angled depositions in Innotec of 100nm has optimal etching in MRC for 600 seconds (10minutes) at Ar gas at 15sccm, chamber pressure 12mT, RF power at 70W, and peak voltage at 660V.

Results have been collected together in the table below for a single angled Innotec deposition of 50nm of gold. For all results, Argon pressure was at 15 sccm and chamber pressure was set to 12 mTorr. Key for the table is as follows

- NG means "no gold" was seen on the surface of the structure and gold is still present on the sidewalls
- NE means "nonuniform etching" was found on the sidewalls of the structures
- TGL means "thin gold layer" was found on the surface of the structure
- NTGL means "nano thin gold layer" was found on the surface of the structure

RF Power	Etch Time	Visible Detection	SEM
100W	6 min 30 sec	NG	NE
100W	5 min	NG	NE
80W	5 min	NG	NE
70W	3 min	TGL	TGL
70W	3 min 30 sec	TGL	TGL
70W	3 min 40 sec	TGL	TGL
70W	3 min 50 sec	NG	NTGL
70W	4 min	NG	NTGL
70W	5 min	NG	NG

Other parameters were also changed to see their effect on the sidewall etch rate such as decreasing the chamber pressure between 5-12mTorr. It was found in general that a lower chamber pressure resulted in longer necessary etch times for the samples

to achieve the sidewall deposition with a clean surface that we desired. However we aimed to minimize etch times and did not pursue a thorough analysis on lower chamber pressures and required etch rates. We did confirm that for pressures below 12mTorr and keeping all other variables constant (power, etch rate, Ar pressure) more gold was present on the surface than with a chamber pressure of 12mTorr.

### 3 Results

We analyzed the profile of the step coverage on a Scanning Electron Microscope (SEM) for the metal deposited through the e-beam evaporator (Innotec) and the sputtering deposition system (Metalica).

#### 3.1 Metalica Results

Fig. 10 shows the profile of one such deposition in Metalica. As evident in this figure, metal on the left sidewall is discontinuous and patchy. Furthermore, we witnessed irregularities in the sidewall coverage between different edges of the nanostructures as evident in the discrepancy in the metal profile on the left and right edge in Fig. 10, and different parts of the wafer in Fig. 11.

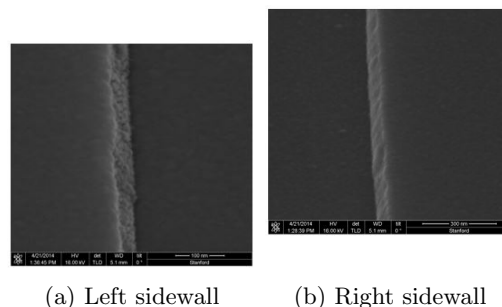
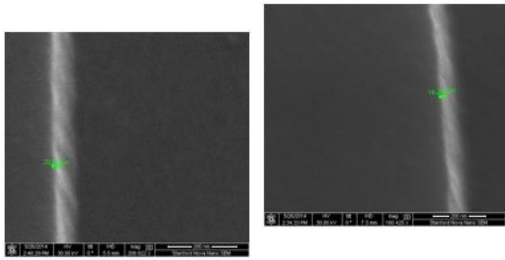


Figure 10: Metal deposited in Metalica

#### 3.2 Innotec Results

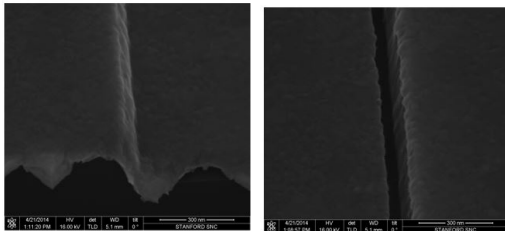
Unlike Metalica, the e-beam metal evaporation performed through Innotec resulted in a much conformal sidewall coverage as evident in Fig. 12a. Fig.



(a) Left side wall in the center of the wafer (b) Left side wall on the top of the wafer

Figure 11: Comparison of Metal deposited in Metalica on two different points on the wafer

12 shows the profile of one such single-sided deposition. Since it was just a single sided deposition, metal was deposited only on one sidewall. Fig. 12b shows that the other sidewall doesn't have metal on it. Furthermore, the dark area in the figure is the horizontal surface where metal wasn't deposited due to shadowing from the sidewall.



(a) Left sidewall (b) Right sidewall

Figure 12: Metal deposited in Innotec

A more detailed SEM image of the right sidewall is shown in Fig.13. Using the width of the shadowed region and the 170nm step height, we can ascertain the incidence angle of metal deposition in innotec in the configuration shown in Fig 3. Fig 14 shows the result of this simple trigonometric calculation and the incidence angle is estimated to be about  $14^\circ$  from the normal.

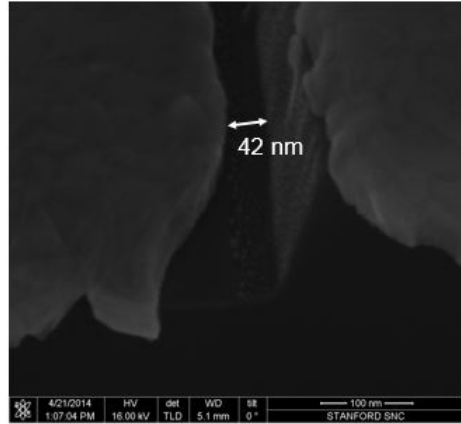


Figure 13: An SEM image of the sidewall on which metal wasn't deposited in Innotec. Clear shadowing from the sidewall can be seen.

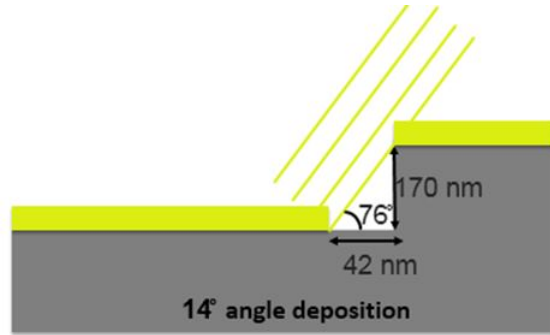


Figure 14: Using the shadowing from a one sided metal deposition, the angle of incidence of Gold atoms is estimated using simple trigonometric identities.

## 4 Gold Enhanced Particle Sorting

### 4.1 Waveguide fabrication

Waveguides were fabricated in the following manner: (1) A bare silicon wafer was thermally oxidized to grow a two micron oxide layer, (2) high stress nitride was deposited using LPCVD, (3) 0.7 micron of photoresist was deposited on the wafer, (4) wafer

was patterned in ASML, (5) nitride was etched in Amtetcher using program four, (6) photoresist was removed.

## 4.2 Sidewall Metal Deposition

Use the procedure detailed in the previous section for fabricating silicon nitride waveguides, two types of waveguides were fabricated. The first waveguide had a width of 400 nm and a height of 350 nm (WG1). The second waveguide had a width of 10 microns and a height of 200 nm (WG2).

WG1 consisted of three specific patterns: (a) straight waveguide, (b) slight bend, and (c) curve around patterns. We aimed to see how our sidewall metal deposition methodology would work with each of the cases. Fig 15 shows a successful gold sidewall deposition with WG1-straight. For this device, a double innotec deposition of gold followed by a 10 minute MRC etch was conducted. From this point on, system parameters are always RF power 70W, Argon 15 sccm, and chamber 12mTorr unless otherwise stated.

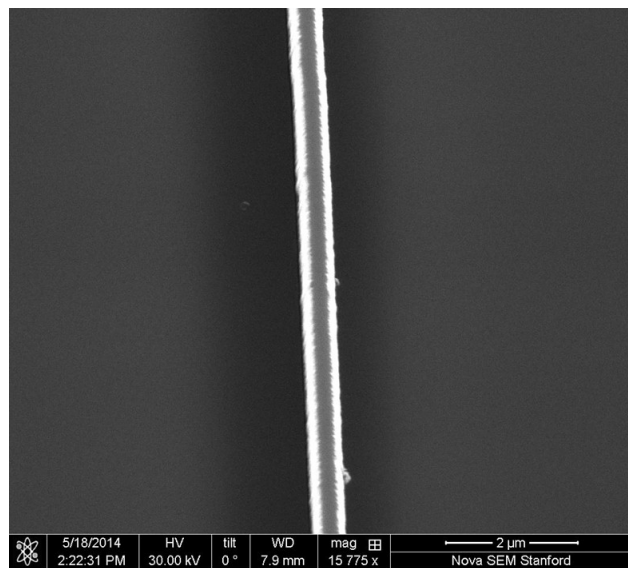


Figure 15: Successful gold sidewall deposition of 50 nm on WG1-Straight

Using the same procedure as detailed above, we found successful sidewall depositions for WG1-slight

bend and WG1-curve. We were unable to exactly characterize what the sidewall thickness was of these structures due to the angle at which we cut our samples for SEM imaging. However, from Fig 16 and Fig 17 we are able to confirm that gold has been successfully deposited onto the sidewalls of the structure.

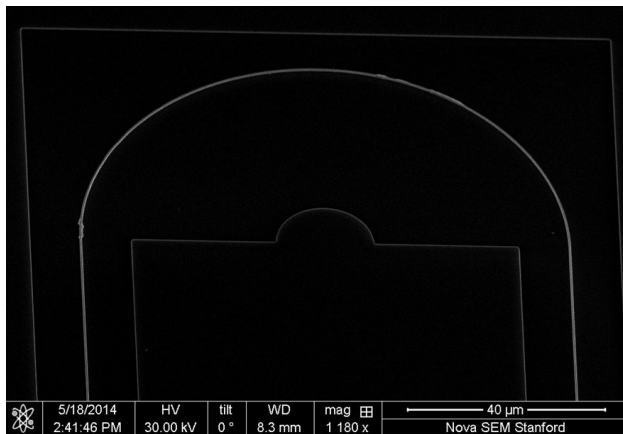


Figure 16: Successful gold sidewall deposition on a fully bended waveguide structure

WG2 only consisted of straight waveguides with a width of 10 microns and a height of 200 nm. Without gold sidewalls, these waveguides are used to propel microparticles down the waveguide strip using the evanescent field protruding out of the top of the silicon nitride cladding layer. An image of the waveguide with microparticles sitting on the surface is shown in Fig. 18

Successful 50 nm sidewall metal deposition was achieved with WG2 as well as shown in Fig. 19. The gold sidewalls had a significant contribution to the attenuation of the evanescent field down the waveguides. This effect shows potential abilities to separate glass particles of two different sizes.

This effect is shown specifically for a 4 micron and 8 microns bead as shown in Fig. 20. A 2.5 micron spot size emerges from the tapered lensed fiber (1550nm) with a 14 micron working distance. We used glass beads suspended in distilled water. The suspensions were pipetted onto the waveguide until the entire waveguide was fully covered with liquid. Propulsion of the particles was observed using a CMOS camera

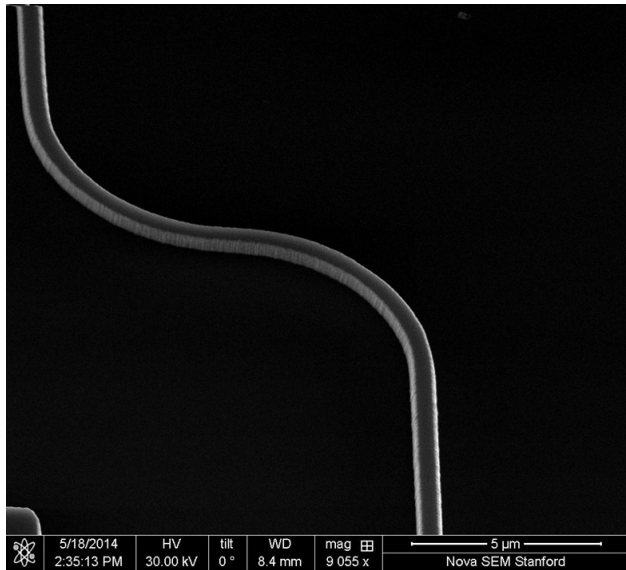


Figure 17: Successful gold sidewall deposition on a waveguide structure with a slight bend

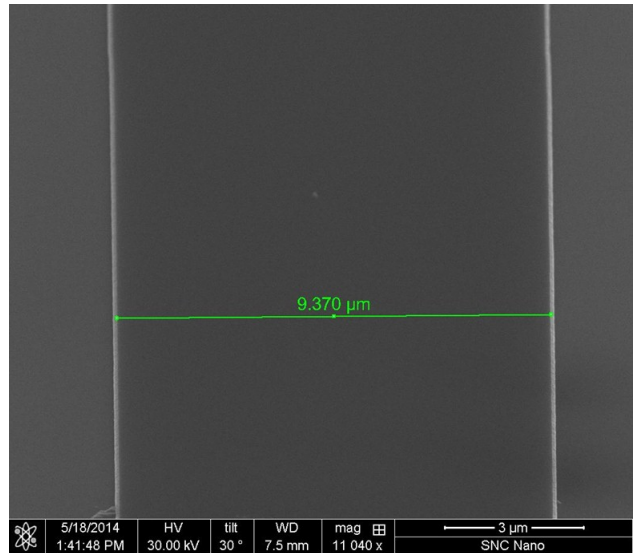


Figure 19: Image of 10 micron beads sitting on top of surface that contains a 10micron wide SiN waveguide strip

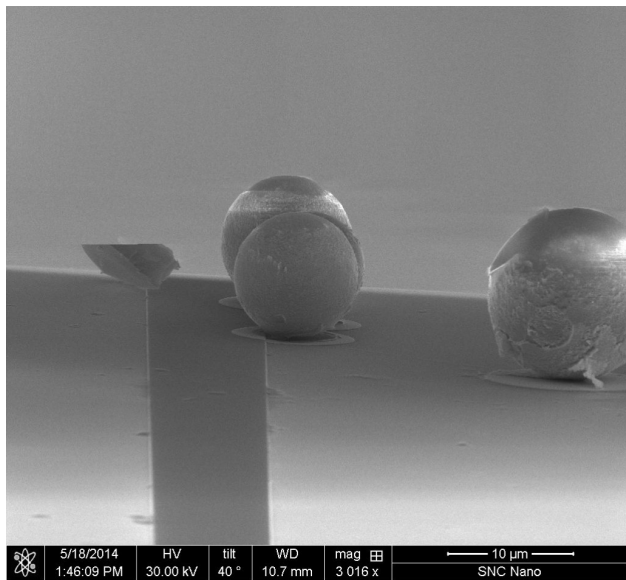


Figure 18: Image of 10 micron beads sitting on top of surface that contains a 10micron wide SiN waveguide strip

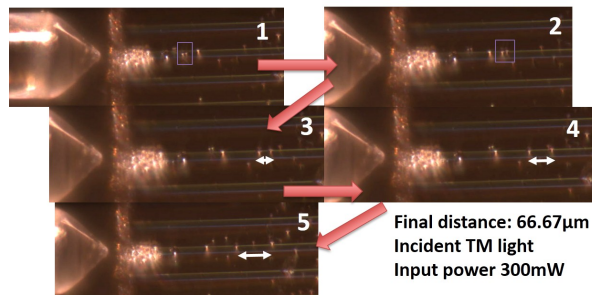


Figure 20: Particle separation between 4 micron and 8 micron glass particles due to sidewall attenuation. Particles are separated by 67microns.

and a 50X objective lens (NA is 0.42). For an input power of 300mW with incident TM light at 1550nm, it took 2 minutes for the 4 and 8 micron beads to fully separate and come to a stop on the guide.

This method holds potential to be integrated with microfluidic structures to automate and sort between cells of various sizes. The gold sidewalls provide the waveguide structure with the necessary attenuation to separate particles of various sizes along the device.



## 5 Enhanced emission in Ge

Due to its applications in CMOS compatible optical interconnect network, Ge lasers has been of significant interest. Donguk et al. have developed a Ge nanobeam pseudo-hetrostructure that allowed them to achieve carrier confinement in strained Ge [4]. Using this technique they saw photoluminescence from their Ge nanobeams [5]. While these nanostructures show photoluminescence, the emission is not high and can be improved by the surface plasmon polaritons.

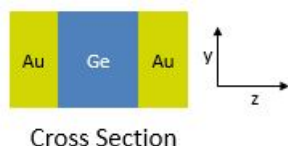


Figure 21: Cross section of the Ge nanobeam structure that was simulated in an FDTD simulator. It's infinite in the x direction.

We found that if we sandwich Germanium with Gold on the sides, we can get significant enhancement in emission. The structures that was numerically simulated in Lumerical FDTD solver is shown in Fig.21. As evident in Fig. 22, simulations show that we get about a 900x emission enhancement at about 1950nm just because of Gold on the sidewalls.1950nm is the wavelength around which strained Ge emits [4].

Using the mechanisms mentioned earlier in this paper, Gold can be deposited on the sidewall of these nanobeams and this emission enhancement can be achieved experimentally.

### 5.1 Conclusion

We investigated and characterized a technique for vertical sidewall metal deposition through the use of angled mounts in Innotec and Ar sputter etching in the MRC. We demonstrate sidewall metal deposition for two different materials: germanium nanorods and silicon nitride strip waveguides. The applicability of this deposition technique can be extended to other applications as well based on the techniques showed in this paper. This represents the first such experimental demonstration of sidewall metal deposition.

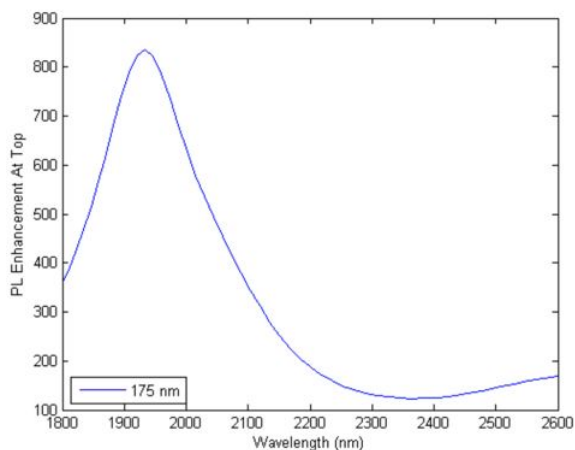


Figure 22: Simulation showing about 900x emission enhancement at about 1950nm.

## References

- [1] P. Vettiger, P. Buchmann, K. Dätwyler, G. Sasso, and B. VanZeghbroeck, “Nanometer sidewall lithography by resist silylation,” *Journal of Vacuum Science & Technology B*, vol. 7, no. 6, pp. 1756–1759, 1989.
- [2] E. Cheng, H. Zou, Z. Yin, P. Jurčiček, and X. Zhang, “Fabrication of 2d polymer nanochannels by sidewall lithography and hot embossing,” *Journal of Micromechanics and Microengineering*, vol. 23, no. 7, p. 075022, 2013.
- [3] W. Eidelloth and R. Sandstrom, “Wet etching of gold films compatible with high  $t_c$  superconducting thin films,” *Applied physics letters*, vol. 59, no. 13, pp. 1632–1634, 1991.
- [4] D. Nam, D. S. Sukhdeo, J.-H. Kang, J. Petykiewicz, J. H. Lee, W. S. Jung, J. Vuckovic, M. L. Brongersma, and K. C. Saraswat, “Strain-induced pseudoheterostructure nanowires confining carriers at room temperature with nanoscale-tunable band profiles,” *Nano letters*, vol. 13, no. 7, pp. 3118–3123, 2013.
- [5] D. Nam, D. Sukhdeo, S.-L. Cheng, A. Roy, K. C.-Y. Huang, M. Brongersma, Y. Nishi, and

K. Saraswat, "Electroluminescence from strained germanium membranes and implications for an efficient si-compatible laser," *Applied Physics Letters*, vol. 100, no. 13, p. 131112, 2012.